J. Fluid Mech. (1982), *vol.* 125, *pp.* 347–358
Printed in Great Britain

Nonlinear analysis of cavity flows around arbitrarily shaped bluff bodies in a constrained flow

By K. SATO

Department of Mechanical Engineering, Kanazawa Institute of Technology,
7–1, Ogigaoka Nonoichimachi, Ishikawa 921, Japan

(Received 3 March 1982)

This paper presents a new nonlinear analytical method based on the Fourier-series expansion for cavity flows, by which we can systematically deal with curved bodies of arbitrary shape. Furthermore, in the present study, the momentum defect within the cavity wake is reasonably well estimated by the displacement effect through the momentum theorem. For two-dimensional symmetric flows around various bluff bodies, theoretical predictions are shown quantitatively and compared with experimental data, wherever possible.

1. Introduction

A high-speed body moving through a liquid inevitably brings about a cavitating or a supercavitating flow, so that analysis of the phenomenon is one of the most important problems in fluid mechanics. The problem of cavity flows, even when only the inviscid flow outside the ensuing cavity-wake system is of interest, is still difficult because of their highly nonlinear nature. In the case of inviscid flows, the partially cavitating or the supercavitating flows can be solved by the free-streamline theory.

Only in the special case of flows around slender bodies or thin hydrofoils with small incidence angles has the simpler linear theory been developed, and its usefulness is attested by many investigators (see, for example, Tulin & Burkart 1955; Oba 1961). However, the cavity flows around bluff bodies need a nonlinear analysis, in which there are some unsolved problems on account of their nonlinear nature arising from the nonlinear free-surface condition and an unknown location of the free boundary. A nonlinear solution is generally difficult to obtain with the exception of a few cases: the flows around inclined flat plates and wedges with various vertex angles. Therefore, we need a simpler nonlinear method analysing the cavity flow around an arbitrarily curved body.

In this respect, Wu & Wang (1964) proposed the integral iteration method using a set of functional equations of the Villat type for curved bodies in steady plane flows. Though this method has been applied successfully to several cavitating-flow problems (Furuya 1973), there seems scope for improvement in the rate of the convergence and the complexity of the iterative procedure.

In the present study, the nonlinear method is further developed by replacing the shape of the wetted body surface with the Fourier series (with coefficients a_n), and basic equations for the cavity-flow problems are reduced to a set of nonlinear functional equations including the shape coefficients a_n. This method can deal systematically with bodies of arbitrary shape. In such cavity flows, it is necessary to estimate the cavity and the cavity wake connected with cavity drag. Though there are some cavity-flow models that can represent finite cavities, the existing cavity

models differ appreciably from each other for flows around bluff bodies in solid walls, as stated by Wu (1972). Most of these models contain unreasonable assumptions for the momentum defect in the viscous far wake. In order to make the cavity-flow analysis more physically realistic, it is necessary to estimate the cavity wake (that is, the far wake) reasonably. The present study uses a method based on the momentum theorem through the concept of the displacement thickness. The inviscid-flow theory considering the displacement effect of the cavity wake may be valid for analysis of the cavity flow. This model was proposed in the linearized super-cavitating theory by Oba (1969) and developed for the nonlinear theory by Sato (1981).

It is the purpose of this paper to present a new nonlinear analytical method in which curved bodies of arbitrary shape can be systematically dealt with by means of a Fourier-series expansion, and also to present a cavity-flow theory that adequately takes into account the displacement effect of the cavity wake and satisfies the condition of conservation of momentum. For a normal plate, wedges, circular cylinders and parabolic bodies, theoretical predictions are made quantitatively and compared with experiments.

2. Mathematical formulation of the problem

Consider the cavity flow around an arbitrarily shaped body of base-chord length $h = 1$, in a two-dimensional water tunnel of width t with rigid walls, as depicted in figure 1. The streamlines on the body surface separate from points A and A', so that a fully developed cavity or a partially developed cavity in the time-averaged steady state follows the body. A static pressure is assumed to be almost constant in the cavity region. Furthermore, the cavity-wake region with a velocity defect exists behind the cavity region of length l_x. We denote the uniform upstream flow velocity as $q_1 = 1$, the infinite downstream velocity as q_2 and the wetted surface length from the leading stagnation point to the cavity separation point as S. In order to deal with the cavity wake within the limits of potential theory, the wake is replaced by the displacement surface with the representative surface velocity q_2.

A physically important parameter known as the cavitation number σ is defined as

$$\sigma_1 = \frac{2(p_1 - p_c)}{\rho q_1^2}, \tag{1}$$

where p_1 and p_c are respectively the pressures at upstream infinity and inside the cavity and ρ is the density of the fluid medium.

Assuming the flow to be irrotational, there exists a complex potential $f = \phi + i\psi$, where ϕ and ψ are respectively the velocity potential and stream function. Then the flow field in the z-plane is shown as a slit f-plane depicted in figure 2 (a). The upper-half f-plane is mapped onto the upper-half ζ-plane as shown in figure 2 (b) by the mapping function:

$$f = \frac{t}{2\pi} \log\left(1 + \frac{\zeta}{m}\right), \tag{2}$$

where the real parameter m is the ξ-coordinate corresponding to the point I at upstream infinity.

This flow problem in the ζ-plane is reduced to a so-called mixed boundary-value

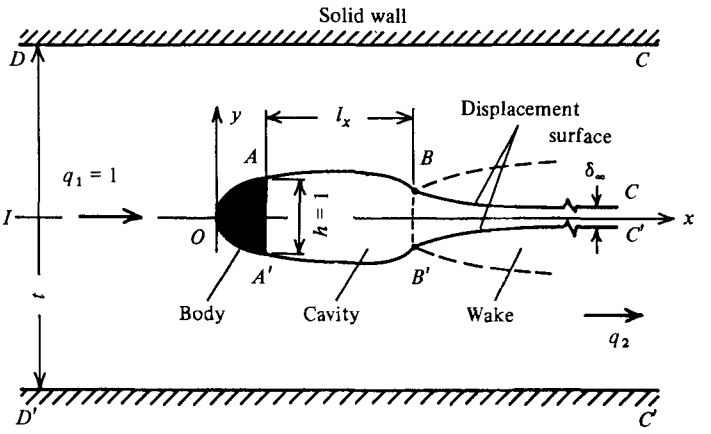

FIGURE 1. Flow configuration in the physical $z = x+iy$ plane. The cavity wake is replaced by the displacement surface with the surface velocity q_2.

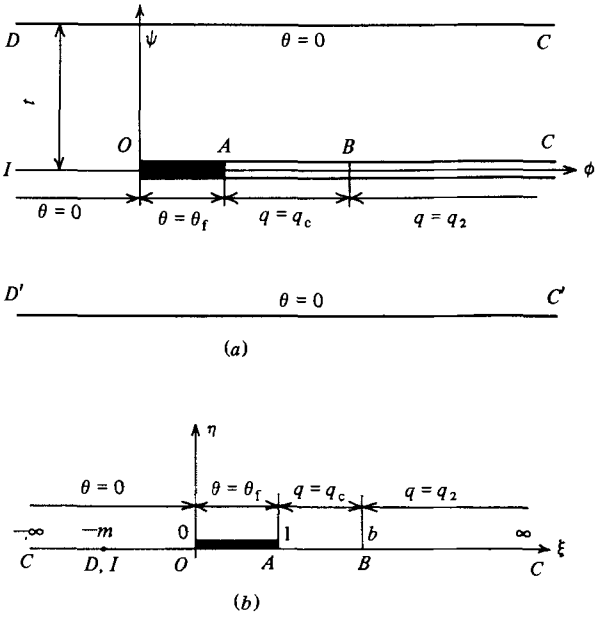

FIGURE 2. Flow configurations are (*a*) the potential $f = \phi+i\psi$ plane and (*b*) the transformed $\zeta = \xi+i\eta$ plane together with boundary conditions.

problem, of which all boundary conditions are expressed in terms of either the real or imaginary part of the logarithmic complex velocity:

$$\omega(\zeta) = \log\frac{q}{q_2} - i\theta.$$

The boundary conditions are expressed as

$$\theta = 0 \quad (-\infty < \xi < 0), \quad \theta \equiv \theta_f \quad (0 < \xi < 1), \tag{3a, b}$$

$$q \equiv q_c \quad (1 < \xi < b), \quad q = q_2 \quad (b < \xi < \infty), \tag{3c, d}$$

where θ_f is the flow direction on the wetted body surface, $q_c = (1+\sigma)^{\frac{1}{2}}$ is the velocity of the cavity surface, and b is the ξ-coordinate corresponding to the cavity closure point B. Taking account of the condition that $\omega(\zeta)$ has a branch point at $\xi = 1$, we can choose an auxiliary function $i(\zeta-1)^{\frac{1}{2}}$. According to the method of the Riemann–Hilbert problem (see Muskhelishvili 1953), the solution of the present problem is obtained as

$$\omega(\zeta) = \frac{i}{\pi}(\zeta-1)^{\frac{1}{2}}\left\{\int_0^1 \frac{\theta_f d\nu}{(1-\nu)^{\frac{1}{2}}(\nu-\zeta)} - \log\left(\frac{q_c}{q_2}\right)\int_1^b \frac{d\nu}{(\nu-1)^{\frac{1}{2}}(\nu-\zeta)}\right\}. \tag{4}$$

3. The solution of the problem

3.1. *Treatment of the body shape*

In order to treat a body of arbitrary shape, the inclination of the wetted body surface is expressed by the Fourier sine series

$$\theta_f(\xi) = \pi\theta_0 + \sum_{n=1}^{\infty} a_n \sin n\theta, \tag{5}$$

$$a_n = \frac{2}{\pi}\int_0^{\pi} (\theta_f - \pi\theta_0)\sin n\theta \, d\theta, \tag{6}$$

where $$\xi = 1-\sin^4 \tfrac{1}{2}\theta \quad (0 < \theta < \pi).$$

θ_0 is given by the body shapes at the leading stagnation point $\xi = 0$ and the cavity separation point $\xi = 1$ as

$$\theta_0 = \theta_1 + \xi\theta_2, \tag{7}$$

where the constants θ_1 and θ_2 are

$$\theta_1 = \frac{\theta_f(0)}{\pi}, \quad \theta_2 = \frac{\theta_f(1)-\theta_f(0)}{\pi}.$$

3.2. *Unknown parameters*

Although the solution is given by (4), the parameters σ (or q_c), q_2, m, b and a_n ($n = 1, 2, \ldots, N$) in the equation remain undetermined. If the parameter b is chosen as an external one, the number of unknown parameters is $N+3$. Therefore $N+3$ conditions are required.

The first condition is that at upstream infinity $\xi = -m$. Since $q = q_1 = 1$ at this point, the first equation is written using (4) as

$$F_1 = q_2^{1-\theta_m} q_c^{\theta_m}\left(\frac{a-1}{a+1}\right)^{\theta_0} \exp\left\{\sum_{n=1}^{N} a_n[(-1)^n(a^{\frac{1}{2}}-(a-1)^{\frac{1}{2}})^{2n} - ((a+1)^{\frac{1}{2}}-a^{\frac{1}{2}})^{2n}] - 2\theta_2 a\right\} - 1 = 0, \tag{8}$$

where

$$a = (m+1)^{\frac{1}{2}}, \quad \theta_m = \frac{2}{\pi}\arctan\frac{b-1}{m+1}.$$

The second condition is obtained from the condition of conservation of momentum. In the case of two-dimensional symmetrical flow, the condition of momentum conservation is necessary only in the direction of the undisturbed flow, though a two-dimensional flow generally needs two conditions, as stated by Sato (1981). As the existence of a velocity defect in the cavity wake is equivalent to the superposition of inflow towards the body on the uniform stream, replacing the cavity wake with

the displacement surface of the surface velocity q_2 is associated with a sourcelike contribution to the inviscid flow field, the strength of the effective source being $Q = q_2\delta_\infty$, where δ_∞ is the displacement thickness at downstream infinity (see Batchelor 1967). Therefore, when the momentum theorem is applied to a large control surface around the body and cavity, including this source with the momentum $\rho Q q_2$, the drag coefficient C_{Df} on the body is given by

$$C_{\mathrm{Df}} = \frac{2D_{\mathrm{f}}}{\rho q_1^2 h} = C_{\mathrm{D}\infty} + C_Q = t(q_2-1)(3q_2-1), \tag{9}$$

where D_{f} is the drag exerted on the body and $C_{\mathrm{D}\infty}$ is the drag coefficient exerted on the semi-infinite body consisting of the cavitating body, cavity and cavity wake:

$$C_{\mathrm{D}\infty} = t(q_2-1)^2, \quad C_Q = \frac{2\rho Q q_2}{\rho q_1^2 h} = 2tq_2(q_2-1), \quad \delta_\infty = \frac{t(q_2-1)}{q_2}$$

from the condition of continuity. On the other hand, the drag coefficient C_{Df} is also given by the pressure integral on the body surface:

$$C_{\mathrm{Df}} = \frac{4}{\rho}\int_0^{\frac{t}{2}} (p-p_{\mathrm{c}})\,dy = q_{\mathrm{c}}^2 - \frac{t}{\pi}\int_0^1 \frac{q\sin\theta_{\mathrm{f}}}{m+\xi}\,d\xi. \tag{10}$$

Since (9) obtained on the control surface should be equal to (10) on the body surface, the following equation is obtained:

$$F_2 = q_{\mathrm{c}}^2 - \frac{t}{\pi}\int_0^1 \frac{q\sin\theta_{\mathrm{f}}}{m+\xi}\,d\xi - t(q_2-1)(3q_2-1) = 0. \tag{11}$$

The third condition is given by a scaling between the physical z-plane and the transformed ζ-plane. The scaling is determined by the correspondence between the cavity separation point A and $\xi = 1$ in the ζ-plane. Since the relation between the z- and f-planes is

$$df = q\exp(-i\theta)\,dz,$$

and on the streamline $d\psi = 0$, then

$$dz = \frac{1}{q}\exp(i\theta)\left(\frac{d\phi}{d\xi}\right)d\xi. \tag{12}$$

Defining s to be the arclength of the wetted part of the body measured from the front stagnation point O, we can obtain the following relation on the wetted body surface:

$$dz = \exp(i\theta_{\mathrm{f}})\,ds.$$

Combining this equation with (12), we can write

$$s(\xi) = \int_0^\xi \frac{1}{q}\left(\frac{d\phi}{d\nu}\right)d\nu = \frac{t}{2\pi}\int_0^\xi \frac{d\nu}{(m+\nu)q}. \tag{13}$$

Then the third equation is obtained as

$$F_3 = s(1) - S = 0, \tag{14}$$

where S denotes the total arclength of the wetted portion.

The fourth condition is related to the shape parameters a_n. In the case of the bodies with θ_{s} = constant like a normal plate and wedges, three equations (8), (11) and (14)

are sufficient to obtain solutions. However, in the case of curved bodies, the fourth equation is necessary. From (6),

$$F_{n+3} = a_n - \frac{2}{\pi}\int_0^\pi (\theta_f - \pi\theta_0)\sin n\theta\, d\theta = 0, \tag{15}$$

where $n = 1, 2, \ldots, N$. As the direct relation between the physical plane z and the transformed plane ζ are unknown *a priori* we should pay attention to the fact that $\theta_f(\xi)$ is a function of q_c, q_2, m and a_n.

Finally, we can rearrange (8), (11), (14) and (15) as follows:

$$F_i(q_c, q_2, m, a_1, \ldots, a_N) = 0, \tag{16}$$

where $i = 1, 2, \ldots, N+3$. This system of $N+3$ nonlinear equations F_i should be solved for the solutions $x_i = (q_c, q_2, m, a_1, \ldots, a_n)$. In the present analysis, they can be solved by a Newton–Raphson iteration procedure. That is, (16) is rewritten as

$$\left(\frac{\partial F_i}{\partial x_j}\right)_0 x_j = \left(\frac{\partial F_i}{\partial x_j}\right)_0 (x_j)_0 - (F_i)_0, \tag{17}$$

where $j = 1, 2, \ldots, N+3$ and the Einstein summation convention is used. The suffix 0 indicates known quantities. If we give $(x_j)_0$ to start the above iteration procedure, we can find x_j from (17). Then the iteration should be continued until a convergent set of x_j is found. In order to save computing time, the calculation of $(\partial F_i/\partial x_j)_0$ should be neglected in the iteration after the solutions x_j converge to some extent.

3.3. *Basic characteristics of the flow*

The cavitation number σ is given using (1) as

$$\sigma_1 = q_c^2 - 1. \tag{18}$$

Dividing (4) into real and imaginary parts for $0 < \xi < 1$, we obtain the velocity distribution on the body:

$$q_f(\xi) = q_2^{1-\theta_b} q_c^{\theta_b}\left[\frac{1-(1-\xi)^{\frac{1}{2}}}{1+(1-\xi)^{\frac{1}{2}}}\right]^{\theta_0} \exp\left\{\sum_{n=1}^{N} a_n[\cos n\theta - ((1+\sin^2\tfrac{1}{2}\theta)^{\frac{1}{2}} - \sin\tfrac{1}{2}\theta)^n] - \theta_2 \sin^2\tfrac{1}{2}\theta\right\}, \tag{19}$$

where

$$\theta_b = \frac{2}{\pi}\arctan\frac{b-1}{1-\xi}.$$

From (9) or (10), the drag coefficient C_D can be obtained:

$$C_D = C_{Df}. \tag{20}$$

From the imaginary part of (4) for $1 < \xi < b$, the inclination of cavity surface is given as

$$\theta_c = \theta_0[\pi - 2\arctan(\xi-1)^{\frac{1}{2}}] - 2\theta_2(\xi-1)^{\frac{1}{2}} + \sum_{n=1}^{N} a_n I_n + \frac{1}{\pi}\log\left(\frac{q_c}{q_2}\right)\log\frac{(b-1)^{\frac{1}{2}} - (\xi-1)^{\frac{1}{2}}}{(b-1)^{\frac{1}{2}} + (\xi-1)^{\frac{1}{2}}}, \tag{21}$$

where

$$I_n = -\frac{1}{\pi}(\xi-1)^{\frac{1}{2}}\int_0^1 \frac{\sin n\theta}{(1-\nu)^{\frac{1}{2}}(\nu-\xi)}\, d\nu.$$

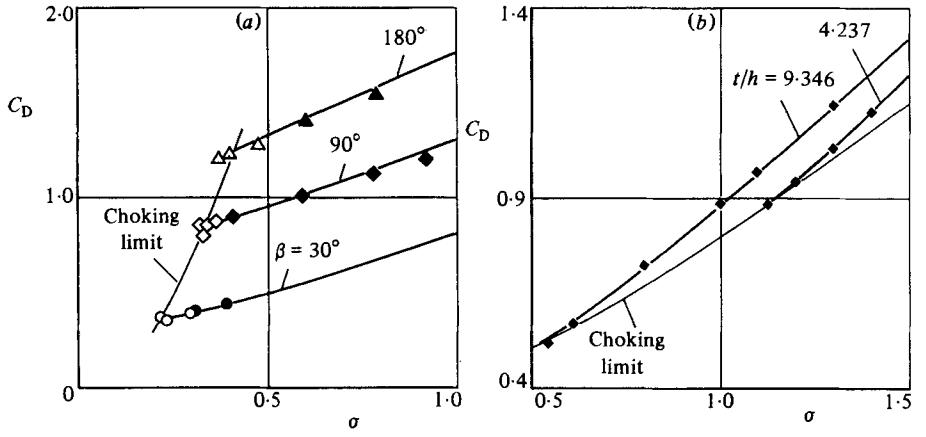

FIGURE 3. Comparison of the drag coefficients for wedges with the vertex angles β. (*a*) compares with the experiment: ○, ●, $\beta = 30°$; ◇, ◆, 90°; △, ▲, 180°; the open symbols are for developed cavities and the solid ones are for partial cavities. (*b*) compares with the Riabouchinsky model for $\beta = 30°$: ◆, Riabouchinsky model; ——, present theory.

The cavity shape $z_c = x_c + iy_c$ is given from (12) and (21) as

$$z_c(\xi) = z_s + \frac{t}{2\pi q_c}\int_1^{\xi} \frac{\exp i\theta_c}{m+\nu}\, d\nu, \tag{22}$$

where z_s is the position of the cavity separation point in the z-plane. Therefore the cavity closure point z_l connected with the cavity length is given by $z_l = z_c(b)$.

4. Numerical results and discussion

4.1. *Normal plate and wedges*

In order to examine the wall effects on the cavitating flows and the validity of the present method, which makes a reasonable consideration of momentum defect within the cavity wake, some representative numerical computations were made for a normal plate and wedges of various vertex angles. In these cases, since $a_n = 0$ and θ_f = constant, the three functional equations (8), (11) and (14) were used and the computer execution time was very short.

In figure 3 (*a*), the present results are compared with the experimental data of Waid (1957) for the drag coefficients C_D. This figure indicates that the present solutions can favourably simulate the experimental data in not only the supercavitating region but also the partially cavitating one. Wu, Whitney & Brennen (1971) conducted a comparison between existing cavity models for the pure drag exerted on the body in a constrained flow and found that the prediction based on the Riabouchinsky model was typically superior to them. Figure 3 (*b*) shows a comparison of the present solutions with the results of Wu *et al.* for a wedge of vertex angle $\beta = 30°$. As the difference between these two results is very small, the displacement effect of the cavity wake seems to be small in the pure-drag problem.

Figure 4 shows the present solutions for the various channel-width to base-chord ratios t/h and wedge vertex angles β. Figure 5 shows the relation between the cavity length l_x/h and the cavitation number σ. It shows also the results from replacing the condition of (11) with the zero wake width $\delta_\infty = 0$ at downstream infinity. This

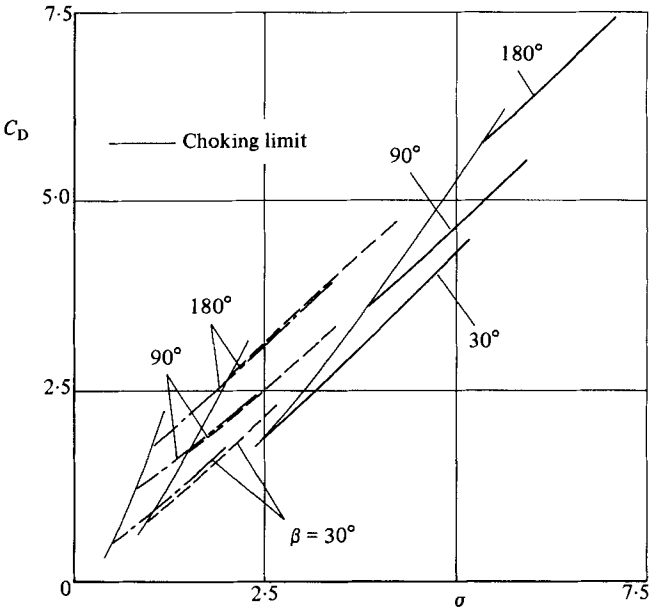

FIGURE 4. Wall effects on the drag coefficients of wedges for various β and t/h: ——, $t/h = 2{\cdot}5$; – – –, $= 5$; – · –, $= 10$; ——, choked flow.

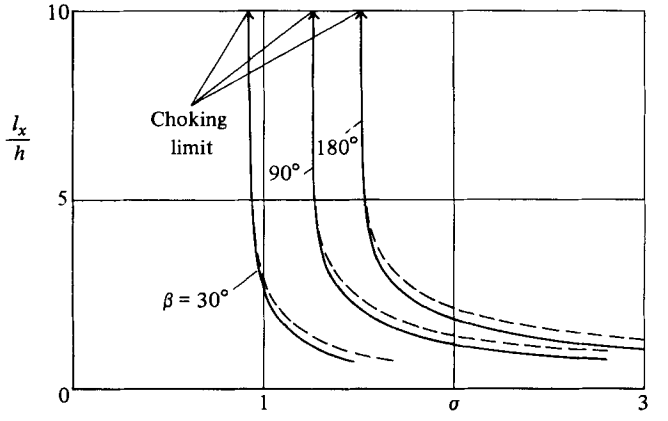

FIGURE 5. Wall effects on the cavity length of wedges for $t/h = 5$, based on the different theoretical models: ——, present model; – – –, double-spiral model.

condition $\delta_\infty = 0$ is equivalent to that of the double-spiral model of Tulin (1964). Only when the cavity length becomes rather shorter, do the results based on these two models differ from each other. These figures show that, even when the cavity lengths are comparatively short, the gradient l_x to σ is very steep, and the flow is effectively choked owing to the wall effect. Therefore it follows that the fully developed supercavitating flow is limited within the very narrow region, in a constrained flow with solid walls.

4.2. *Curved bodies of arbitrary shape*

As examples of curved bodies, numerical computations were conducted for cylindrical and parabolic bodies. A set of nonlinear equations shown by (16) was solved by the

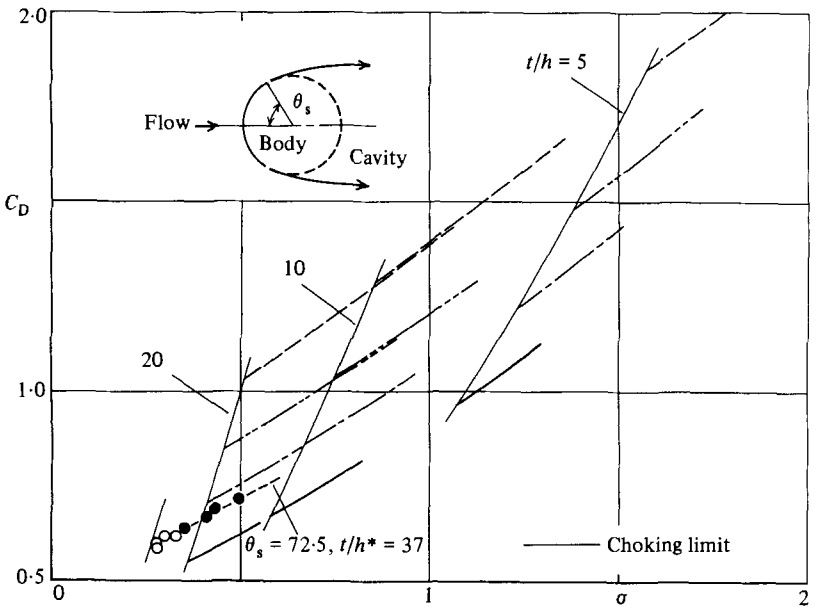

FIGURE 6. Drag coefficients of circular cylinders for various separation angles θ_s. Theory: – – –, $\theta_s = 45°$; – – – –, 60°; – – –, 70°; ——, 80°; ——, choked flow. Experiment: ○, ●, $t/h^* = 37$, where h^* = diameter of the cylinder, the open symbols are for developed cavities and the solid ones are for partial cavities.

Newton–Raphson method, in which the computer execution time depended greatly on starting values. When the parameters a_n, q_c, m and q_2 had not yet been obtained for a curved body, the solutions q_c, m, q_2 for a wedged body and $a_n = 0$ were used as the starting values. The calculation of the cavitation number σ and the drag coefficient C_D required only the term number $N = 5$ at most for any shape, but that of the pressure coefficient required more terms in the case of parabolic bodies with larger bluffness. It should be mentioned that the convergence of the numerical computation was relatively stable and fast: for example, for $N = 5$ the execution time within 90 s on an IBM 4341 was required when the results of another curved body were used as the starting values, and about 200 s when the results of a wedge were used. Of course, the convergence greatly depends on the algorithm of the computation program and may be improved.

4.2.1. *Circular cylinder.* The cavity separation angles θ_s were assumed *a priori* and were chosen as 45°, 60°, 70° and 80°. The inclination θ_f of the body wetted surface is written as

$$\theta_f = \tfrac{1}{2}\pi - 2s \sin \theta_s, \tag{23}$$

and therefore

$$\theta_1 = \tfrac{1}{2}, \quad \theta_2 = -\frac{\theta_s}{\pi}.$$

In figure 6, the drag coefficients C_D are shown for various t/h and σ. Waid's experimental data are also shown for reference. Though the separation angle θ_s during the experiment is unknown, the present solution for $\theta_s = 72{\cdot}5°$ and $t/h^* = 37$ shows a good agreement with these experimental data in a wide range, including a choking point.

Figure 7 shows the pressure distributions $C_p = 2(p - p_1)/\rho q_1^2$ for $\theta_s = 60°$, 80° and $t/h = 5$, 20. It is found that the peak near the minimum point of the pressure

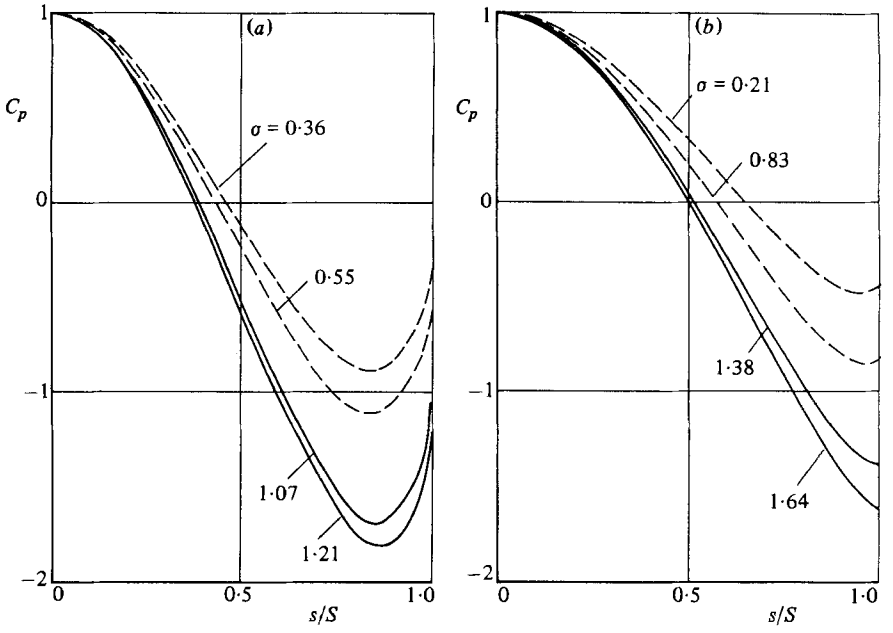

FIGURE 7. Pressure distributions on circular cylinders for various σ and t/h: ---, $t/h = 20$; ——, 5. (*a*) corresponds to $\theta_s = 80°$ and (*b*) to $\theta_s = 60°$.

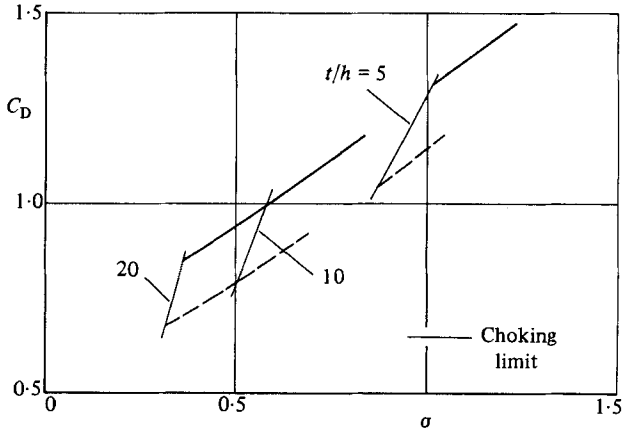

FIGURE 8. Drag coefficients of parabolic bodies for various t/h and k: ——, $k = 1$; ---, 1·5; ——, choked flow.

coefficient C_p becomes sharper as t/h increases. In the case of θ_s = constant, the position of the minimum point moves upstream as the cavitation number σ decreases, but the extent of the movement is very small. From the viewpoint of the inviscid theory, the separation point should be determined by the smooth separation conditions ($d\omega/d\zeta \to 0$, $\zeta \to 1$, as stated by Wu 1972) for a smoothly curved body, but it is known that considerable discrepancy really exists between the theoretical predictions and the observed results (see Brennen 1969). Since the separation phenomenon is due to viscous effects, the separation point θ_s depends on the Reynolds number R as well as the cavitation number σ. The separation point $\theta_s = 80°$ used here corresponds to that of the experiment ($t/h = 20$, $R = 1{\cdot}9 \times 10^5$) of Oba, Ikohagi

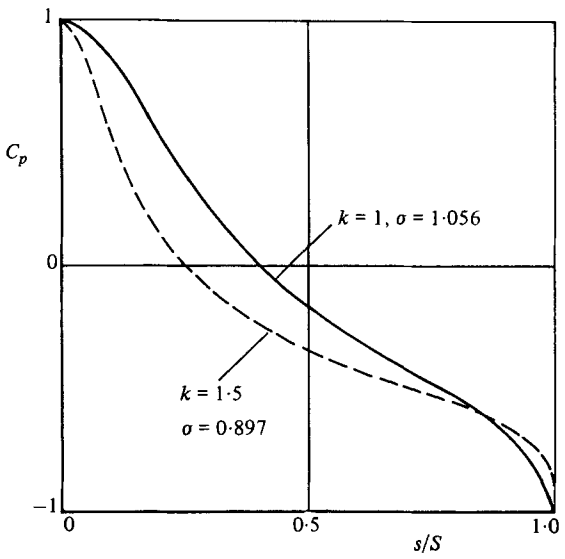

FIGURE 9. Pressure distributions on parabolic bodies for various k.

& Yasu (1980), and $\theta_s = 60°$ to that near the smooth separation condition, as indicated in the pressure distributions of figure 7 (*b*). On the other hand, Yamaguchi & Kato (1981) proposed an iteration procedure that regards a laminar boundary-layer separation point as a cavity separation point, where the laminar separation point is calculated from the pressure distribution obtained by the inviscid potential theory. It should also be possible to apply this procedure to the present method.

4.2.2. *Parabolic bodies.* The shapes $ky_f = x^{\frac{1}{2}}$ of parabolic bodies are expressed as

$$\theta_f = \tfrac{1}{2}\pi - \arctan 2kx^{\frac{1}{2}}, \tag{24}$$

and therefore

$$\theta_1 = \tfrac{1}{2}, \quad \theta_2 = -\frac{1}{\pi}\arctan k^2.$$

Figures 8 and 9 show representative examples of the drag coefficients C_D and the pressure distribution C_p. The number of shape coefficients a_n is chosen as $N = 15$ in the calculation of C_p. When the bluffness of the body increases (that is, k decreases), C_D becomes larger and the choking limit line moves towards larger σ.

5. Concluding remarks

Taking account of momentum defect in the cavity wake, a nonlinear analysis of cavity flows is made for the two-dimensional flows around arbitrary bluff bodies in constrained flows with solid walls. The drag coefficients, the pressure distributions and other properties are obtained quantitatively for a normal plate, wedges, parabolic bodies and circular cylinders with various separation angles. As the present method is not directly dependent on body shape, we can deal systematically with cavitating bodies of arbitrary shape. The present method can also be applied to hydrofoils of arbitrary shape in the unbounded flows as well as to cascade flows.

The author wishes to express his gratitude to Professor Risaburo Oba for his advice and encouragement.

REFERENCES

BATCHELOR, G. K. 1967 *An Introduction to Fluid Dynamics*. Cambridge University Press.

BRENNEN, C. 1969 *Cavitation State of Knowledge*. A.S.M.E.

FURUYA, O. 1973 Numerical computations of supercavitating hydrofoils of parabolic shape with Wu and Wang's exact method. *California Institute of Technology Rep.* E-79A.15.

MUSKHELISHVILI, N. I. 1952 *Singular Integral Equations*. Noordhoff.

OBA, R. 1961 Linearized theory of supercavitating flow through an arbitrary form hydrofoil. *Z. angew. Math. Mech.* **41**, 354–363.

OBA, R. 1969 A study on finite cavity supercavitating blocked flow. *Rep. Inst. High Speed Mech., Japan* **20**, 345–371.

OBA, R., IKOHAGI, T. & YASU, S. 1980 Supercavitating cavity observations by means of laser velocimeter. *Trans. A.S.M.E.* I: *J. Fluids Engng* **102**, 433–440.

SATO, K. 1981 Nonlinear analysis of supercavitating cascade performance by condition of conservation of momentum. In *Proc. 9th Turbomachinery Conf.* pp. 7–12 (in Japanese).

TULIN, M. P. 1964 Supercavitating flows – small perturbation theory. *J. Ship Res.* **7**, 16–37.

TULIN, M. P. & BURKART, M. P. 1955 Linearized theory for flows about lifting foils at zero cavitation number. *David W. Taylor Model Basin Rep.* C-638.

WAID, R. L. 1957 Water tunnel investigation of two-dimensional cavities. *California Institute of Technology Rep.* E-73.4.

WU, T. Y. & WANG, D. P. 1964 A wake model for free-streamline flow theory. Part 2. Cavity flows past obstacles of arbitrary profile. *J. Fluid Mech.* **18**, 65–93.

WU, T. Y., WHITNEY, A. K. & BRENNEN, C. 1971 Cavity-flow wall effects and correction rules. *J. Fluid Mech.* **49**, 223–256.

WU, T. Y. 1972 Cavity and wake flows. *Ann. Rev. Fluid Mech.* **4**, 243–284.

YAMAGUCHI, H. & KATO, Y. 1981 A study on a supercavitating hydrofoil with rounded nose. *J. Soc. Naval Arch. Japan* **149**, 83–149 (in Japanese).